Extra-tropical atmospheric response to equatorial Atlantic cold tongue anomalies

Reindert J. Haarsma and Wilco Hazeleger

Royal Netherlands Meteorological Institute (KNMI)

P.O. Box 201

3730 AE De Bilt

The Netherlands

haarsma@knmi.nl

Submitted to Journal of Climate

Revised version

October 2006

Abstract

The extra-tropical atmospheric response to the equatorial cold tongue mode in the Atlantic Ocean has been investigated with the coupled ocean-atmosphere model SPEEDO. Similar as in the observations the model simulates a lagged co-variability between the equatorial cold tongue mode during late boreal summer and the east Atlantic pattern a few months later in early winter. The equatorial cold tongue mode attains its maximum amplitude during late boreal summer. However, only a few months later, when the ITCZ has moved southward, it is able to induce a significant upper tropospheric divergence which is able to force a Rossby wave response. The lagged co-variability is therefore the result of the persistence of the cold tongue anomaly and a favorable tropical atmospheric circulation a few months later. The Rossby wave energy is trapped in the South Asian subtropical jet and propagates circumglobal before it reaches the North Atlantic. Due to the local increase of the Hadley circulation, forced by the cold tongue anomaly, the subtropical jet over the North Atlantic is enhanced. The resulting increase in the vertical shear of the zonal wind increases the baroclinicity over the North Atlantic. This causes the non-linear growth of the anomalies due to transient eddy-feedbacks to be largest over the North Atlantic, resulting in an enhanced response over that region.

1. Introduction

Sea surface temperatures (SSTs) in the tropical Atlantic are dominated by two modes of variability: The meridional gradient mode and the equatorial cold tongue mode (Hastenrath 1978; Ruiz-Barradas et al. 2000). The meridional gradient mode is primarily driven by latent heat fluxes and can be largely explained as a result of direct atmospheric forcing, without the need to invoke a significant role for local unstable air-sea interactions or ocean circulation (Czaja et al. 2002). Using observations and an intermediate coupled model the mechanism of the equatorial cold tongue mode was first investigated by Zebiak (1993). He hypothesizes that the mechanism of the equatorial cold tongue mode is essentially the same as of the El-Niño mode in the Pacific. Both modes are being caused by the "Bjerknes-Feedback", with a crucial role for the ocean dynamics. An important difference between these two modes are the stability characteristics: El-Niño is the result of unstable air-sea interactions, whereas the cold tongue mode is thought to be a stochastically forced damped mode (Zebiak 1993, Carton and Huang 1994). A comprehensive overview of tropical Atlantic variability has been given by Xie and Carton (2004).

Using NCEP/NCAR reanalysis (Kalnay et al. 1996) Czaja and Frankignoul (2002) found, with the Maximum Covariance Analysis (MCA) analysis, that the North Atlantic horseshoe interannual SST anomaly in summer and fall (The seasons refer to the Northern Hemisphere in this paper.) was associated with the North Atlantic Oscillation

(NAO) in early winter. Their analysis also suggested that the early winter NAO was also influenced by the Atlantic equatorial cold tongue mode in late summer and early fall. Because their analysis suffered from the constraint of spatial orthogonality of the covariance patterns, Frankignoul and Kestenare (2005) redid the analysis by using rotated MCA patterns. In addition they removed the ENSO teleconnections prior to the analysis and extended the NCEP/NCAR reanalysis with 5 year. The new analysis confirms the relation between the NAO pattern and the horseshoe SST anomaly, but denies the effect of the equatorial cold tongue mode on the NAO. Instead they found a weak relationship between the equatorial cold tongue mode during SON and a 500 hPa pattern during Nov.-Dec. (NDJ) that is similar to the eastern Atlantic pattern (Wallace and Gutzler 1981).

The relation between the equatorial cold tongue mode and the Northern Hemisphere atmospheric circulation has also been investigated with atmospheric general circulation models (AGCMs) coupled to an ocean mixed layer model or forced by prescribed SSTs. Both Drevillon et al. (2003) and Peng et al. (2005) found a significant response over the North Atlantic and Western Europe. They differ however in the mechanism responsible for this response. Drevillon et al. (2003) argue that a positive phase of the equatorial cold tongue mode reinforces convection over the Amazon, inducing an anomalous divergence in the upper troposphere, which initiates a Rossby wave train over the North Atlantic. In Peng et al. (2005) the response to the warm phase of the cold tongue mode is enhanced convection over the central tropical Atlantic. The linear Rossby-wave train induced by this anomalous convection appears to be very different from the simulated nonlinear response. This brings Peng et al. (2005) to the

conclusion that the transient-eddy feedbacks are fundamental for the extra-tropical response, which is supported by the results of Watanabe and Kimoto (1999).

Although observational as well as atmospheric modeling studies suggest a weak but significant response to the equatorial cold tongue mode over the North Atlantic and Western Europe, important aspects of the physical mechanism are still unclear. Two main questions emerge:

1. What is the cause of the time lag in the atmospheric response?
2. How is the energy transferred from the Atlantic tropical region toward the North Atlantic and Western Europe?

Recently a realistic simulation of the tropical Atlantic variability using the coupled ocean-atmosphere model SPEEDO was obtained by Hazeleger and Haarsma (2005). The realistic simulation of the equatorial cold tongue mode makes SPEEDO a suitable tool for investigating the extra-tropical response to this mode. SPEEDO is only fully coupled over the Atlantic basin. Outside this region prescribed SSTs are used as a lower boundary condition for the atmospheric model. This configuration eliminates the influence of other oceans on the North Atlantic variability and concentrates on the tropical Atlantic-Northern Hemisphere connection.

We will first investigate whether the coupled model is able to simulate the observed relationship between equatorial cold tongue mode and the atmospheric circulation over the North Atlantic. As will be shown below the coupled model indeed simulates to a large extend the observed relationship. We will then subsequently concentrate on the two main questions formulated above by performing idealized

experiments with the atmosphere model coupled to an ocean mixed layer model forced with an anomalous heat flux in the tropical Atlantic diagnosed from the coupled experiment.

The main argument for this approach in contrast to using an atmosphere model forced with observed SSTs is that there the heat fluxes at the air-sea interface do not need to be realistic. This induces unrealistic simulated atmospheric variability (Bretherton and Battistsi 2000, Sutton and Mathieu 2002). The cold tongue mode in the coupled model is shifted 10^{o} eastward with respect to the observations and therefore may affect the resultant atmospheric teleconnections. In addition the inter tropical convergence zone (ITCZ) moves too far south during winter and spring in the model. However, the good simulation of the observed relationship between the cold tongue mode and the atmospheric circulation by the coupled model indicates that the atmospheric teleconnections are not crucially affected by these deficiencies.

The structure of the paper is as follows. In section 2 the model is described. The equatorial cold tongue mode simulated by SPEEDO is discussed in section 3. In section 4 the relationship between the cold tongue mode and the atmospheric circulation over the North Atlantic is explored. A discussion of the results and the conclusions are presented in section 5.

2. Model

The coupled atmosphere-ocean model that we use in this study is nicknamed SPEEDO (Speedy-Ocean). It consists of an atmospheric primitive equation model (Speedy) with a vertical resolution of 7 layers and a truncation at wave number 30. The model has simplified physics, which makes it computationally inexpensive. A five layer version of the model is described in detail by Molteni (2003). The 7 layer version has improved climate and is described and validated in Hazeleger et al. (2003) and Bracco et al. (2004). The ocean component consists of the Miami Isopycnic Coordinate Ocean Model (MICOM) version 2.7 (Bleck et al. 1992). The model uses potential density as a vertical coordinate. It consists of 22 layers and has a horizontal resolution of 1 degree. The MICOM model is configured for an Atlantic basin from 40^{o}S to 60^{o}N. At the lateral boundaries in the north and south the thermodynamic properties of the model are restored towards observations (Levitus et al. 1998). The Levitus data has also been used to initialize the ocean model. Outside the Atlantic basin and over land climatological surface temperature is specified. This model configuration is the same as used by Hazeleger and Haarsma (2005), hereafter HH2005.

As shown in HH2005, SPEEDO gives a good representation of both the tropical Atlantic climatology, with a correct simulation of the zonal gradient of the tropical Atlantic thermocline, and tropical variability including the meridional gradient mode and the cold tongue mode. Also the extra-tropical variability and teleconnections are

simulated qualitatively well (Molteni 2003, Hazeleger et al. 2003, Sterl and Hazeleger 2005). Therefore SPEEDO is a very suitable tool for investigating the extra-tropical response to the cold tongue mode.

In addition to SPEEDO we will also use a model configuration in which the atmospheric component of SPEEDO (Speedy) is coupled to a passive ocean mixed layer model over the Atlantic. The mixed layer depth is 50 m. To ensure that the climatology of the mixed layer model stays close to the climatology of the coupled model an implied divergence of the ocean heat transport is included in the temperature equation for the mixed layer. The implied divergence of the ocean heat transport is diagnosed from a run with the atmosphere model in which the climatological SST of the coupled model is used as the lower boundary condition. This heat flux is called a "Q-flux.". Details of the mixed layer model and the "Q-flux" experiment can be found in Haarsma et al. (2005) and Hazeleger et al. (2005). Similar as in SPEEDO, SSTs are prescribed outside the Atlantic basin.

3. Atlantic equatorial cold tongue mode variability

In the 80 year simulation described by HH2005, the model accurately simulates the zonal gradient of the tropical Atlantic SSTs and the thermocline depth (Figs. 7 and 8 in HH2005). It simulates also realistic modes of tropical Atlantic coupled variability. The dominant mode of variability obtained by rotated empirical orthogonal functions (REOFs) describes temperature variations in the equatorial cold tongue and is related to changes in the equatorial zonal wind stress. It explains 16% of the variance. The second mode of variability (12%) displays temperature variations of the northern tropical

Atlantic and is related to anomalous cross equatorial winds. Fig. 1a shows the SSTs of the cold tongue mode computed from monthly mean anomalies, which are defined as the deviations from the mean annual cycle. Compared with the equatorial cold tongue mode as derived from observations by Ruiz-Barradas et al. (2000), the maximum in the SST pattern is shifted 10 degrees to the east being located closer to the African coast. Also the negative SSTs east of Brazil and the positive SSTs along the North African coast are not observed. Apart from these relatively small differences, the SST pattern shows a good correspondence with the observed SST pattern. Figs. 1bc show the regression of the principle component (PC) of the equatorial cold tongue mode onto precipitation and wind stress. The maximum of the precipitation in the central Atlantic is located south of the equator, whereas in the observations it is located at the equator (Ruiz-Barradas et al. 2000). This southward displacement is also observed in the wind stress. The reason for this southward displacement of the atmospheric response is the too southerly location of the ITCZ in the model. This is a common problem in many atmospheric GCMs as recently discussed by Biasutti et al. (2006). Apart from these deficiencies the cold tongue mode simulated by the model is in good agreement with the observations. Also the amplitude of the SST and the wind stress with a standard deviation of 0.5 ^{o}C and 0.05 Nm^{-2} compare well with the observations (Ruiz-Barradas et al. 2000). The precipitation and wind stress patterns suggest that the equatorial cold tongue mode forces the atmospheric circulation, with low level convergence and rising motion over the positive SST anomaly, thereby supporting the “Bjerknes-Feedback” hypothesis.

The variability of the equatorial cold tongue mode is largest during the boreal late summer as seen in Fig. 2. The maximum occurs during July consistent with observations

(Carton and Huang 1994, Carton et al. 1996). This maximum is related to the seasonal cycle in the eastern tropical Atlantic and the east-west tilt of the equatorial thermocline. The seasonal cycle in SST and wind stress as well as the structure of the thermocline are simulated realistically by the model as shown by Figs. 7 and 9 in HH2005. During the late boreal summer the West African monsoon attains its maximum. The associated surface winds cool the surface and shoal the thermocline in the eastern tropical Atlantic, which reaches its minimum depth during this period. Due to this shallow thermocline, perturbations in the thermocline depth result in larger SST variations.

The time series of the PC of the SST of the equatorial cold tongue for the last 40 years is shown in Fig. 3a. Variations are visible from seasonal to decadal time scales. Individual events are characterized by a time scale in the order of two years. However, a spectral analysis for the whole time series reveals a red spectrum without a significant dominant time scale (Fig. 3b). This suggests that although ocean dynamics appears to be important for this mode, the stochastic forcing by the atmosphere masks any preferential time scale of these ocean processes. The dynamics of the equatorial cold tongue mode will be further explored in a forthcoming paper.

4. Extra-tropical variability related to the equatorial cold tongue mode

In section 4.1 we will first discuss the relationship between the equatorial cold tongue mode variability and the variability of the atmospheric circulation over the North Atlantic in the coupled model. This is a purely statistical analysis. In order to further understand how the equatorial cold tongue mode forces the extra-tropical circulation we performed simulations with the atmospheric model coupled to a mixed layer model in

which an anomalous Q-flux associated with the equatorial cold tongue mode is prescribed. These are described in section 4.2. Finally a 200 member ensemble of Q-flux anomaly experiments with a length of 1 month has been run in order to investigate in detail the temporal development of the atmospheric response to an equatorial cold tongue anomaly. This is described in section 4.3.

4.1 Coupled model

In order investigate whether the relationship between the geopotential height at 500hPa (Z500) and tropical SST as described by Frankignoul and Kestenare (2005) is reproduced in SPEEDO we repeated their lagged MCA analysis on SPEEDO data. Fig. 4a reveals that in SPEEDO the equatorial cold tongue mode in late summer (JAS) is related to an anomalous circulation over the North Atlantic early winter (OND). Although at first sight the atmospheric circulation anomaly is similar to the North Atlantic Oscillation (NAO), it is shifted towards the south east with a strong loading at about 45^{o} N and 20^{o} W, and resembles more the eastern Atlantic pattern described by Wallace and Gutzler (1981). The MCA analysis of SPEEDO is similar as obtained by Frankignoul and Kestenare (2005).

To obtain a global view of the relationship between the equatorial cold tongue mode and the atmospheric circulation we regressed the time series of the principal component for JAS of the equatorial cold tongue mode onto the global Z500 field of OND (Fig. 4b). Similar as for the MCA analysis positive SST anomalies in the eastern tropical Atlantic are related to negative anomalies of Z500 over the North Atlantic. Positive anomalies appear over Eastern Europe. The maximum correlation is obtained

over the North Atlantic and is in the order of 0.3. In addition negative anomalies are seen over the eastern Pacific indicating that the response is not confined to the North Atlantic and European regions. There is also a response in the Southern Hemisphere, with a wave train along 60^{o}S.

4.2 Q-flux experiments

The lagged analysis of the coupled model in section 4.1 suggests that a causal relationship exists between SSTs in the eastern tropical Atlantic during late summer and the North Atlantic and western European atmospheric circulation during late fall and early winter. This is similar as observed. In order to understand the mechanism of this lagged response, we performed an experiment in which the atmosphere is coupled to a mixed layer and is forced with an anomalous heat flux in the tropical Atlantic. This anomalous heat flux is diagnosed from an SST forced run with a prescribed equatorial cold tongue anomaly. In order to get a robust signal the amplitude of this SST anomaly is 2 times the standard deviation. The maximum amplitude of this anomaly is 1^{o} C. The amplitude of the SST anomaly is kept constant throughout the year. This is in contrast to the observed anomaly, which attains its maximum amplitude during late summer. Keeping the amplitude constant provides us information about the sensitivity of the atmospheric response to the seasonal cycle. It should be noted that the anomalous heat flux diagnosed from the constant SST anomaly has a seasonal cycle. The length of the time integration is 100 year. In addition, a control integration of the same length without the heat flux anomaly was performed. The heat flux in the control run was computed

from a 50-yr atmosphere-only run with climatological SSTs from the coupled run. Details of this procedure are described in Haarsma et al. (2005).

4.2.1 Atmospheric response to cold tongue anomaly

The atmospheric response to the anomalous heat flux appears to be strongly dependent on the seasonal cycle. During boreal summer the Northern Hemispheric response is very weak. The response becomes significant during fall and attains its maximum amplitude during winter. The increase in the Z500 response from late summer to early winter is clearly seen in Fig. 5. As for the coupled run the response during OND (Fig. 5c) is characterized by negative Z500 values over the North Atlantic. The positive center over Europe is shifted more to the north and east compared to the coupled run. Despite these differences the agreement between the coupled run and the Q-flux experiment is good. Comparing the results between the first 50 year and last 50 year of the Q-flux experiment reveals that although the gross features of the response are robust, there are still considerable differences due to internal low frequency variability. These differences are comparable to the differences between the coupled run and the Q-flux run. During ASO (Fig. 5a) the response in Z500 is weak and located over the north western part of the North Atlantic. This pattern is similar to the Z500 pattern obtained with an MCA analysis for the coupled run between tropical SST and Z500 for ASO (not shown), confirming that the seasonal dependence in the Q-flux experiment is similar to that in the coupled model.

The seasonal dependence of the extra-tropical response suggests that the lagged covariance in the coupled run can be explained by this seasonal dependence if an

equatorial cold tongue anomaly in the late summer persist until early winter. Indeed the PC of the cold tongue mode in late summer (JAS) is well correlated with the PC in early winter (OND) (correlation of 0.79), whereas the standard deviation of the cold tongue mode during OND is still 70% of that during JAS. For the SST data set of the NCEP/NCAR reanalysis the correlation between JAS and OND for the ATL3 region (15^oW-5^oE, 3^oS-3^oN) is 0.71. The physical mechanism that emerges is that although the cold tongue anomaly attains its maximum during late summer the atmospheric circulation prohibits energy transport to the extra-tropical Northern Hemisphere. Only during early winter the conditions become favorable, whereas the cold tongue mode is sufficient persistent to maintain the characteristics of late summer into early winter. The strongest response in the Q-flux experiment is obtained during the seasons NDJ and FAM. However, during these seasons the equatorial cold tongue mode is weak and its PC no longer well correlated with its PC during late summer.

4.2.2 Physical mechanism of atmospheric response to cold tongue anomaly

In order to facilitate the discussion we will consider here a positive cold tongue anomaly. For a cold anomaly the signs have to be reversed. The anomaly induces a direct circulation in the tropical Atlantic, with rising air above the positive anomaly. The outflow at the top of the tropopause generates an anomalous divergence. Due to this divergence anomalous Rossby waves are generated which can propagate away from the source region (Hoskins and Karoly 1981).

The dynamics of Rossby wave propagation can be understood by analyzing the barotropic vorticity equation applied at the level of maximum divergence, i.e. 200 hPa (Sardeshmukh and Hoskins 1985):

$$\partial\zeta/\partial t + V_\psi \cdot \nabla\zeta = S,$$

where S is the Rossby wave source: $S= -\zeta D - V_\chi \cdot \nabla\zeta = -\nabla.(V_\chi \zeta)$

Here ζ is the absolute vorticity which is the sum of is the relative vorticity ξ and the Coriolis parameter f: $\zeta = f + \xi$. D is the divergence, V_ψ the rotational horizontal velocity, and V_χ the divergent horizontal velocity. The first term $-\zeta D$ of S is the effect of vortex stretching, whereas the second term $- V_\chi \cdot \nabla\zeta$ is caused by the advection of vorticity by the divergent wind.

Figure 6 shows for the Q-flux anomaly experiment the anomalous divergence D at 200hPa for the different months together with the position of the ITCZ. The ITCZ is computed as the line of zero meridional surface wind. The anomalous D is only significant during early winter which explains the absence of an extra-tropical response of the cold tongue mode during late summer. The upper tropospheric divergence is strongly regulated by the position of the ITCZ. In summer the ITCZ is situated north of the cold tongue mode and the stable atmosphere suppresses strong vertical movement and consequently upper air divergence. In agreement the anomalous rainfall response to the cold tongue anomaly is also much smaller during the summer.

The Rossby wave source S shown in Fig. 7 also reveals the seasonal dependence. However, in contrast to D it also has a significant signal over the Sahara and the Middle

East. Although the divergence D induced by the equatorial cold tongue anomaly is the primary source of the Rossby wave propagation, the final solution is strongly modified by $-V_\chi \cdot \nabla\zeta$. The strong signal of $-V_\chi \cdot \nabla\zeta$ over the Sahara and the Middle East indicates that in these regions the atmospheric flow is modified and transformed into a source region for Rossby waves. The Middle East is located near the entrance of the South Asian subtropical jet, which can act as a wave guide for Rossby wave propagation. The strong signal of $-V_\chi \cdot \nabla\zeta$ over the Middle East therefore suggests that part of the Rossby Wave energy might get trapped in the South Asian subtropical jet. This will be explored in section 4.3.

The Rossby wave response in the extra-tropical regions can be modified by transient-eddy feedbacks. To start the analysis of this mechanism, the change in the zonal wind U at 200mb is shown in Fig. 8. It reveals that the change in the upper tropospheric U is mainly confined to the Atlantic sector, with a banded structure consisting of negative anomalies over the tropical Atlantic, positive anomalies over the subtropics and again negative anomalies at the mid latitudes. The easterly anomalies of upper tropospheric U over the tropical Atlantic are caused by the anomalous Walker circulation with a rising branch over the positive cold tongue mode anomaly and a descending branch over eastern Brazil. The increase in the upper tropospheric U at the subtropics is related to the increase in the Hadley circulation over the Atlantic caused by the local forcing of the cold tongue anomaly. Due to the conservation of angular momentum an increase of the Hadley circulation will result in a stronger subtropical jet.

The increase in the subtropical jet will affect the vertical shear in U and thereby the baroclinic activity over the North Atlantic. The Eady Growth Rate Maximum

$$\sigma_{BI} = 0.31\ f\ |\| \partial \mathbf{u}/\partial z \|\ N^{-1},$$

where f is the Coriolis parameter, **u** the zonal wind and N the Brunt-Väisälä frequency, is a suitable measure of baroclinicty (Hoskins and Valdes 1990). It represents the growth rate of the most rapidly growing baroclinic disturbances. Similar as Hoskins and Valdes (1990) we have computed σ_{BI} for the lower troposphere between the levels of 850 and 700 hPa. Figure 9 shows for the Northern Hemisphere σ_{BI} for the control run and the change due to the cold tongue anomaly. The maxima in σ_{BI} for the control run clearly correspond with the main regions of cyclogenesis in the Pacific and Atlantic storm tracks. The change in $\sigma_{BI,}$ due to the cold tongue mode, results in a dipole structure over the eastern Atlantic, with an increase south of the storm track and a smaller decrease north of it. This change in σ_{BI} can be understood by realizing that the region of maximum σ_{BI} is located in the stormtracks, poleward of the subtropical jet. The increase in the subtropical jet will therefore tend to move the region of maximum $\sigma_{BI,}$ towards the subtropics due to of the increase of $\partial \mathbf{u}/\partial z$ in that region. Analysis of the different terms which contribute to the change in σ_{BI} reveals that indeed the dominant term is the vertical shear in U. The contribution of N to variations in σ_{BI} is negligible. Over the Pacific there is hardly any change in σ_{BI} in agreement with the absence of notable changes in the subtropical jet. The simulated changes over the Rockies and the Himalaya, where the 850 hPa geopotential height surface is located beneath the surface, are spurious.

The southward shift in baroclinic activity caused by the increase in the subtropical jet will subsequently induce a southward shift of the polar jet, which is driven by eddy

momentum convergence of baroclinic eddies. This southward shift of the polar jet explains the negative anomalies of U at the mid latitudes in Fig. 8. Lee and Kim (2003) showed in their model that when the Hadley circulation is sufficient strongly enhanced this mechanism is capable to produce a switch from a state with a double jet structure consisting of a subtropical and a polar jet to a state with a single jet structure in which the polar jet is merged with the subtropical jet.

In order to check the above argument we computed the production of zonal mean momentum by the transient-eddy feedback. This is given by the meridional convergence of the zonal mean momentum covariance -d [(u'v')]/dy, where u' and v' are the daily deviations of the monthly mean u and v. The anomalous momentum covariance shows a maximum over the Atlantic storm track region. We therefore assume that this relationship is still approximately valid if we average zonally only over this region. Figure 10 shows for 50^{o}W-25^{o}E, 20^{o}S-70^{o}N the anomalous [u] and -d [(u'v')]/dy*T for OND. T is 14 days thereby assuming that the characteristic time for the adjustment of the circulation to the anomalous transient eddy forcing is in the order of 2 weeks. At about 30^{o}N the zonal wind is enhanced by about 1 m/s, whereas northward of 40 ^{o}N there is a decrease. The structure of the changes in [u] agrees well with - d[(u'v')]/dy*T indicating that the equatorward shift of the jet is driven by a southward shift in baroclinic activity. The main difference is that the increase in [u] at 30^{o}N is considerably larger than the decrease northward of 40 ^{o}N, whereas the absolute value of -d[(u'v')]/dy*T for both regions is about the same. As discussed before this enhanced increase in upper tropospheric U at 30^{o}N is due to the increase of the Hadley circulation, which directly results in an increase of the subtropical jet due to the conservation of angular momentum. The amplitude of

-d [(u'v')]/dy*T is too large, but still of the same order of magnitude. The complete balance for the zonally averaged anomalous zonal wind includes apart from the anomalous zonal momentum covariance also the advection of planetary vorticity by the anomalous meridional circulation fv. The anomalous meridional circulation is an induced circulation which counteracts the effects of the eddies (Holton 2004). Therefore both the omission of the fv term and a shorter adjustment time of 2 weeks might explain the too large amplitude of -d [(u'v')]/dy*T. The same analysis over the Pacific region did not reveal a significant change in [(u'v')] , thereby confirming that the transient-eddy activity is only enhanced over the Atlantic.

4.3 Ensemble experiments

In order to understand the temporal development of the extra-tropical response in SPEEDO, in particular the transition from a linear Rossby wave response to the final nonlinear response including the transient-eddy feedbacks, we performed a 200 member ensemble of 30 day integrations for the month November. The initial conditions for the first of November were obtained from a 200-year control integration. For each member a control integration without a Q-flux anomaly and an integration with a cold tongue Q-flux anomaly of 2 standard deviation was produced. Figure 11 shows the 500 hPa geopotential height response. In the first week a Rossby wave train is formed which propagates in eastward direction. The response is rather symmetric with respect to the equator with the Southern Hemisphere response being somewhat stronger. No response is visible yet over the North Atlantic. During the second week the response reaches the

North American continent and the trough over Europe broadens to the eastern part of the North Atlantic. The amplitude of the response is still less than 1 dm. In the third week the response increases to more than 1 dm and a clear response over the entire North Atlantic develops. This result suggests that the response over the North Atlantic is at least partially due to the circumglobal propagation of the forced Rossby wave and locally enhanced by nonlinear interactions, such as described in section 4.2.

Circumglobal teleconnections have recently been discussed by Branstator (2002). He identifies the existence of a circumglobal wave guide pattern, which was also found by Selten et al. (2004). Branstator hypothesizes that global teleconnections are possible due to the existence of wave guides, where Rossby wave energy can propagate over large distances without significant dispersion of energy. These wave guides and their importance for Rossby wave propagation have been investigated by Hsu and Lin (1992) and Hoskins and Ambrizzi (1993). The most important wave guides are the upper tropospheric jets. Relevant for the response to the cold tongue mode is the South Asian subtropical jet, which has been identified as an important wave guide for transferring energy toward the Pacific Ocean. The wave guide effect of the South Asian jet is clearly seen in Fig. 12a, which shows the ensemble mean anomaly of the non divergent meridional wind V at 300 hPa at day 7. At this point in time the integration the Rossby wave energy has reached the Pacific Ocean. The wave train passes over the Sahara and the Middle East which are the regions with significant amplitudes of the Rossby wave source S (Fig. 7). At the end of the integration period a circumglobal wave train has formed as shown in Fig. 12b.

In section 4.2 it was stated that the increase in the Hadley circulation strengthens the subtropical jet and that the change in the transient eddy activity, resulting from this change in U, shifts the polar jet southward. This is supported by the ensemble experiments which show that over the Atlantic during the first two weeks, when the effect of the transient eddies is still small, only the subtropical jet is increased due to the intensification of the Hadley circulation (Fig. 13a). Thereafter the southward shift of the polar jet due to the meridional convergence of eddy momentum transport is clearly visible (Fig. 13b). The extension of the zonal wind anomalies to the surface in Fig.13b, also indicates a prominent role for the baroclinic eddies in generating these anomalies. In Fig. 13a also is clearly seen the change of U in the tropical Atlantic anomalous due to an anomalous Walker circulation, with upper tropospheric easterlies and lower tropospheric westerlies.

The enhanced baroclinicity in the North Atlantic causes the non-linear growth of the anomalies to be strongest in the North Atlantic region, and explains why the response to the cold tongue anomaly is strongest there although it is located at the end of the circumglobal wave guide.

5. Discussion and conclusions

The atmospheric response to the Atlantic equatorial cold tongue mode as simulated by the coupled SPEEDO model has been investigated. Similar to the observations by Frankignoul and Kestenare (2005) weak co-variability exists between the equatorial cold tongue mode during late boreal summer and the atmospheric circulation over the North Atlantic a few months later. In order to investigate the mechanism we have investigated the response with the atmospheric model coupled to a slab ocean

model. In this experiment the equatorial cold tongue anomaly is kept constant throughout the year enabling us to investigate the seasonal dependence of the atmospheric sensitivity to this anomaly. It appears that only during the winter half year, when the ITCZ is situated over the equatorial cold tongue region, the anomaly is able to generate sufficient large upper tropospheric divergence in order to induce a significant extra-tropical Rossby wave response. The equatorial cold tongue mode on the other hand attains its maximum amplitude during late summer. The persistence of the cold tongue anomaly and the favorable atmospheric conditions in early winter explain the lagged co-variability.

Recently Okumura and Xie (2006) noted from satellite and in-situ data a new Niño like phenomenon in the tropical Atlantic that peaks in November-December. This is not seen in COADS data. According to personal communication by Okumura, prior to 1980, the equatorial SST variance shows a single peak in July, which tends to persist into the following winter (correlation of 0.6). During the recent two decades, on the other hand, the equatorial SST variance peaks one month earlier in June and a distinct secondary peak appears in November-December, which show little correlation with the previous June-July SST variations. This November-December equatorial mode is associated with an extra-tropical anomalous circulation pattern which is very similar to the pattern simulated by SPEEDO.

As discussed before one of the deficiencies of SPEEDO is the too southerly position of the ITCZ. The seasonal dependence of the upper tropospheric divergence forced by the equatorial cold tongue mode may therefore be an artifact of SPEEDO. We checked the response of the tropical Atlantic circulation to the cold tongue mode in the 40-year reanalysis of the ECMWF (ERA40) (Uppala 2005). Fig. 14 shows the correlation

of the ATL3 index, defined as the average of the SST over the region 15°W-5°E; 3°S-3°N with the 200 hPa divergence. The response in the 200 hPa divergence shows a zonal band over the Atlantic which moves equatorward from about 7°N in August to about 2°N in November following the seasonal movement of the ITCZ. During the latter month it is situated over the cold tongue anomaly. The correlation increases from 0.4 in August to 0.6 in November despite the reduction in the amplitude of the cold tongue mode. Also the area increases. This supports the hypothesis that due to the more southerly position of the ITCZ during early winter the equatorial cold tongue mode is more effective in forcing a Rossby wave.

An alternative argument for the lagged response is the seasonal variation in the basic state flow. The Rossby wave propagation from the tropics to the extra-tropics will be blocked if there is a critical latitude where the basic state zonal flow is zero (Hoskins and Ambrizzi 1993, Webster and Holton 1982). In Speedy the upper tropospheric flow over the tropical Atlantic is westerly during late summer. This implies that the weak Northern Hemisphere response to the cold tongue mode during this season is not due to the blocking of Rossby wave propagation from the tropical Atlantic region into the Northern Hemisphere, but solely the result of the weak amplitude of the Rossby wave source. However, inspection of the ERA40 reanalysis data reveals that during late summer the tropical Atlantic is situated in a region of upper tropospheric easterlies, inducing a barrier to wave propagation into the Northern Hemisphere. During fall and winter, for both Speedy and the ERA40 reanalysis, the cold tongue mode is situated in a region of upper tropospheric westerlies, allowing Rossby wave propagation into the extra-tropical regions.

Ensemble experiments with Speedy showed that Rossby wave energy is trapped in the South Asian jet and propagates circumglobal before it reaches the North Atlantic. In order to find evidence for the circumglobal Rossby wave propagation in the observations we computed the regression of the ATL3 index with the ERA40 300 hPa meridional wind V for NDJ. Figure 15 reveals a circumglobal wave train that is very similar to the one simulated by Speedy shown in Fig. 12b, with a corresponding amplitude of 1 m. These results support the hypothesis of a circumglobal response to the equatorial cold tongue mode. A similar circumglobal response by anomalous Indian Ocean SSTs is found by Bader and Latif (2005).

The hypothesis of a circumglobal response to the equatorial cold tongue mode is new. Earlier studies envisage either a direct connection between the tropical and north Atlantic (e.g. Peng et al. 2005), or a connection with convection over the Amazon region (Drevillon et al. 2003, Robertson et al. 2000). Comparing Fig.14 with Fig. 6 reveals that in the ERA40 data the 200hPa divergence is more zonally extended over the central part of the tropical Atlantic, suggesting a greater role for this region in forcing Rossby waves. This indeed implies the possibility of a direct propagation of Rossby waves from the tropical Atlantic into the north eastern Atlantic and Western Europe. Especially during August and September the main response is over the central tropical Atlantic, whereas during October and November, when the ITCZ moves southward toward the Gulf of Guinea, the response becomes more concentrated over this region. As discussed before, during August and September the upper tropospheric divergence in the tropical Atlantic is situated in the easterlies, blocking the propagation of Rossby waves to the extra-tropics. However, in October and November a larger signal could probably propagate

directly to the eastern Atlantic and Western Europe than simulated by Speedy, which has its divergence more concentrated in the eastern tropical Atlantic.

The upper air divergence is caused by rising motion and is in the tropics strongly related to latent heat release due to deep convective precipitation. Precipitation is therefore often used as a proxy for the forcing of the extra-tropical response to a tropical SST anomaly. Correlation of the ATL3 index with the CMAP rainfall data (Xie and Arkin 1996) reveals a significant correlation over the Caribbean and the northern part of the Amazon. This area might therefore be a source for the extra-tropical response induced by the equatorial cold tongue mode as suggested by Drevillon et al. (2003). However the absence of a significant signal in the upper tropospheric divergence has led us to the conclusion that the convection in this region is not deep enough to generate a Rossby wave source.

Both the ensemble experiments and the zonal momentum budget indicate that over the North Atlantic the response is strongly enhanced by the eddy momentum convergence due to transient-eddy feedback, which is confirmed by other studies (Peng et al. 2005, Drevillon et al. 2003). The change in the transient-eddy activity is much larger over the Atlantic than over the Pacific and is related to the local change in the Hadley circulation over the Atlantic induced by the cold tongue mode. This explains why the circumglobal wave response to the cold tongue mode is largest over the Atlantic, although it is at the end of the circumglobal propagation. Because transient-eddy activity is larger during early winter than late summer this is an additional cause for a more prominent response in early winter to the equatorial cold tongue mode as is hypothesized by Peng et al. (2005) as well.

Although the response of the North Atlantic circulation to the cold tongue mode is not very strong it appears to be robust. It is found both in observation and models. Especially in case of a strong cold tongue mode, when its amplitude is more than twice the standard deviation, this opens the possibility to use this relationship for predictions over the North Atlantic and Europe. Figure 4b shows that for a strong cold tongue mode of twice the standard deviation the maximum response in Z500 over the North Atlantic is about 10 m. This is about 10-20% of the standard deviation of the seasonal mean Z500.This suggest that the amplitude of the cold tongue mode in late summer might be a predictor in a forecast system for the North Atlantic for the early winter.

Acknowledgments

We thank Frank Selten and Gerrit Burgers for the helpful discussions and comments on the manuscript. Figure 14 and 15 were made with the Climate Explorer developed by Geert-Jan van Oldenborgh.

References

Bader, J. and M. Latif, 2005: North Atlantic response to an anomalous Indian Ocean SST in a coupled GCM. *J. Climate,* **18,** 5382-5389.

Biasutti, M., A.H. Sobel and Y. Kushnir, 2006: AGCM precipitation biasis in the Tropical Atlantic. *J. Climate*, **19,** 935-958.

Bleck, R., C. Rooth, D. Hu and L.T. Smith, 1992: Salinity-driven thermocline transients in a wind- and thermohaline-forced isopycnic coordinate model of the North Atlantic. *J. Phys. Oceanogr.,* **22,** 1486-1505.

Bracco, A., F. Kucharski, R. Kallummmal and F. Molteni, 2004: Internal variability, external forcing and climate trends in multi-decadal AGCM ensembles. *Climate Dyn.,* **23,** 659-678.

Bretherton, C. S. and D.S. Battisti, 2000: An interpretation of the results from atmospheric general circulation models forced by the time history of the observed sea surface temperature distribution. *Geophys. Res. Lett.,* **27,** 767-770.

Branstator, G., 2002: Circumglobal teleconnenction patterns, the jet stream waveguide, and the North Atlantic Oscillation. *J. Climate,* **15,** 1893-1910.

Carton, J.A. and B. Huang, 1994: Warm events in the tropical Atlantic. *J. Phys. Oceanogr.,* **24,** 888-903.

Carton, J.A. X. Cao, B.S. Giese and A.M. da Silva, 1996: Decadal and interannual SST variability in the tropical Atlantic ocean. *J. Phys. Oceanogr.,* **26,** 1165-1175.

Czaja, A. and C. Frankignoul, 2002: Observed impact of Atlantic SST anomalies on the North Atlantic oscillation. *J. Climate,* **15,** 606-623.

Czaja, A., P. van der Vaart and J. Marshall, 2002: A diagnostic study of the role of remote forcing in tropical Atlantic variability. *J. Climate,* **15,** 3280-3290.

Drevillon, M., C. Cassou and L. Terray, 2003: Model study of the North Atlantic region atmospheric response to autumn tropical Atlantic sea-surface-temperature anomalies. *Quart. J. Roy. Meteor. Soc.,* **19,** 2591-2611.

Frankignoul, C. and E. Kestenare, 2005: Observed Atlantic SST anomaly impact on the NAO: An update. *J. Climate,* **18,** 4089-4094.

Haarsma, R.J., E.J. Campos, W. Hazeleger , A.R. Piola, C. Severijns and F. Molteni, 2005: Dominant modes of variability in the South Atlantic: A study with a hierarchy of ocean atmosphere models. *J. Climate,* **18,** 1719-1735.

Hastenrath S., 1978: On modes of tropical circulation and climate anomalies. *J. Atmos. Sci.,* **35,** 2222-2231.

Hazeleger, W, C. Severijns, R.J. Haarsma, F. Selten, A. Sterl, 2003: SPEEDO-model description and validation of a flexible coupled model for climate studies. KNMI, *Technical Report, TR-257, de Bilt, The Netherlands,* 37 pp.

Hazeleger, W. and R.J. Haarsma, 2005: Sensitivity of tropical Atlantic climate to mixing in a coupled ocean-atmosphere model. *Climate Dyn.,* **25,** 387-399, doi:10.1007/s00382-005-0047-y

Hazeleger, W., C. Severijns, R. Seager en F. Molteni, 2005: Tropical Pacific-driven decadal energy transport variability. *J. Climate,* **18,** 2037-2051

Holton, J.R, 2004: An introduction to dynamical meteorology. Fourth edition, Elsevier Academic Press, London, UK. ISBN:0-12-354015-1, 535pp.

Hoskins, B.J. and D.J. Karoly, 1981: The steady linear response of a speherical atmosphere to thermal and orographic forcing. *J. Atmos. Sci.,* **38,** 1179-1196.

Hoskins, B.J. and P.J. Valdes, 1990: On the existence of storm tracks. *J. Atmos. Sci.,* **47,** 1854-1864.

Hoskins, B.J. and T. Ambrizzi, 1993: Rossby wave propagation on a realistic longitudinally varying flow. *J. Atmos. Sci.,* **50,** 1661-1671.

Hsu, H.-H., and S.-H. Lin, 1992: Global teleconnections in the 250mb streamfunction field during the Northern Hemisphere winter. *Mon. Wea. Rev.,* **120,** 1169-1190.

Kalnay, E. et al., 1996: The NCEP/NCAR 40-year reanalysis project. *Bull. Amer. Meteor. Soc.,* **77,** 437-471.

Lee, S. and H.-K. Kim, 2003: The dynamical relationship between subtropical and eddy-driven jets. *J. Atmos. Sci,* **60,** 1490-1503.

Levitus, S., T.P. Boyer, M.E. Conkright, T. O'Brien, J. Antonov, C. Stephens, L. Stathoplos, D. Johnson, R. Gelfeld, 1998: NOAA Atlas NESDIS 18, WORLD OCEAN DATABASE 1998: Vol 1: Introduction. US Government Printing Office, Washington DC, 346 pp.

Molteni, F., 2003: Atmospheric simulations using a GCM with simplified physical parameterizations. I: model climatology and variability in multi-decadal experiments. *Climate Dyn.,* **20,** 175-191.

Okumura, Y and S.-P. Xie, 2006: Some overlooked features of tropical Atlantic climate leading to a new Niño-like phenomenon. *J. Climate* (in press).

Peng, S., W.A. Robinson, S. Li, and M. Hoerling, 2005: Tropical Atlantic SST forcing of coupled North Atlantic seasonal responses. *J. Climate,* **18,** 480-496.

Robertson, A. W., C.R. Mechoso and Y.-J. Kim, 2000: The influence of Atlantic sea surface temperature anomalies on the North Atlantic Oscillation. *J. Climate,* **13,** 122-138.

Ruiz-Barradas A., J.A. Carton and S. Nigam., 2000: Structure of interannual-to-decadal climate variability in the Tropical Atlantic Sector. *J. Climate,* **13,** 3285-3297.

Sardeshmukh, P. and B.J. Hoskins, 1985: Vorticity balances in the tropics during the 1982-83 El Nino-Southern Oscillation event. *Quart. J. Roy. Meteor. Soc.,* **111,** 261-278.

Selten, F.M., G. Branstator, M. Kliphuis en H.A. Dijkstra, 2004: Tropical origins for recent and future Northern Hemisphere climate change, 2004: *Geophys. Res. Lett.,* **31,** doi:10.1029/2004GL020739

Sterl, A. en W. Hazeleger, 2005: Tropically and extratropically forced atmospheric variability. *Geophys. Res. Lett.,* **32,** L18716, DOI:10.1029/2005GL023757.

Sutton, R. and P.-P. Mathieu, 2002: Response of the atmosphere-ocean mixed-layer system to anomalous heat flux convergence. *Quart. J. Roy. Meteor. Soc.,* **128,** 1259-1275.

Uppala, S.M. and co-authors, 2005: The ERA-40 re-analysis. *Quart. J. Roy. Met. Soc.,* **131,** 2961-3012.

Watanabe, M. and M. Kimoto, 1999: Tropical-extratropical connection in the Atlantic atmosphere-ocean variability. *Geophys. Res. Lett.,* **26,** 2247-2250.

Wallace, J.M. and D.S. Gutzler, 1981: Teleconnections in the geopotential height field during the Northern Hemisphere winter. *Mon. Wea. Rev.,* **109,** 784-812.

Webster, P.J. and J.R. Holton, 1982: Cross-equatorial response to middle-latitude forcing in a zonally varying basic state. *J. Atmos. Sci.,* **39,** 722-733.

Xie, P. and P.A. Arkin, 1996: Analyses of global monthly precipitation using gauge observations, satellite estimates, and numerical model predictions. *J. Climate,* **9,** 840-858.

Xie, S-P and J.A Carton, 2004: Tropical Atlantic Variability: Patterns, Mechanisms, and Impacts. In: *Earth Climate: The Ocean-Atmosphere Interaction*. Geophysical Monograph, AGU, Washington DC.

Zebiak, S.E., 1993: Air-sea interaction in the equatorial Atlantic region. *J. Climate,* **6,** 1567-1586.

Figure Captions

Fig. 1. Regression of the principle component (PC) of the equatorial cold tongue mode onto SST [^{0}C] (a), precipitation [mm day^{-1}](b) and wind stress[Nm^{-2}] (c). The patterns are normalized to one standard deviation of the PC. In this and following figures the solid and dashed contours indicate positive and negative values respectively. The zero contour is omitted.

Fig. 2. Annual variation of the standard deviation of the PC of the equatorial cold tongue mode. The PC is normalized to one standard deviation.

Fig. 3. **a**: Time series of PC of the SST of the cold tongue mode during the last 40 years. **b**: Spectrum of **a** for the entire integration period of 80 years (black dots) together with the fitted AR(1) (red noise) process spectrum (solid line) and the 95% a priori confidence level (dashed line). The PC is normalized to one standard deviation.

Fig. 4. **a**: Lagged MCA analysis of the 80-yr coupled run of tropical SST [^{0}C] (homogeneous map) during JAS (shaded) and Z500 [m] (heterogeneous map) during OND (contours). The explained variance is 46% and the cross correlation is 0.40
b: Regression of the PC of the cold tongue mode of JAS onto the Z500 [m] of OND. The SST time series of the MCA analysis and the PC of the cold tongue mode are normalized to one standard deviation.

Fig. 5. Z500 response in [m] to a 2 stdv anomaly of the cold tongue mode in the Q-flux experiment. The response is averaged over ASO (a), SON (b), OND(c), NDJ(d).

Fig. 6. Anomalous divergence [10^{-6} s^{-1}] at 200 hPa in the Q-flux experiment during ASO(a), SON(b), OND(c) and NDJ(d). The solid line is the position of the ITCZ, which is computed as the line of zero meridional surface wind.

Fig. 7. Anomalous Rossby wave source S [10^{-11} s^{-2}] at 200 hPa in the Q-flux experiment during ASO(a), SON(b), OND(c) and NDJ(d).

Fig. 8. Anomalous zonal wind U at 200 hPa [m] in the Q-flux experiment for OND.

Fig. 9. Maximum Eady Growth rate σ_{BI} in 0.1 day^{-1} in the Q-flux experiment. Control (shaded) and anomalous (contours). Regions where the 850 hPa geopotential height is beneath the surface have been blacked out.

Fig. 10. Anomalous zonal wind u [m s^{-1}] (shaded) and meridional convergence of eddy momentum transport -d (u'v')/dy * T [m s^{-1}] (contours) zonally averaged over the Atlantic (50^{o}W-25^{o}E, 20^{o}S-70^{o}N). T is 14 days.

Fig. 11. Ensemble mean Z500 response [m] (200 members) of a positive cold tongue anomaly of 2 standard deviations in November: **a:** averaged over day 6-10 after the perturbation is switched on; **b:** as a but now averaged over day 11-15 ; **c:** as a but now averaged over day 26-30.

Fig. 12. Ensemble mean response of the non divergent v [m s^{-1}] at 300 hPa at day 7 (upper panel) and averaged over the period 16-30 days (lower panel).

Fig. 13. Ensemble mean response of the zonal wind u [m s^{-1}] zonally averaged over the Atlantic (50^{o}W-25^{o}E, 20^{o}S-70^{o}N) averaged over day 11-15 (**a**) and day 26-30 (**b**).

Fig. 14. Correlation of the ATL3 index with the 200 hPa divergence (ERA40 reanalysis) for the months August till November.

Fig. 15. Regression of the ATL3 index with the ERA40 merdional 300 hPa wind [m s^{-1}] for the period NDJ.

a b

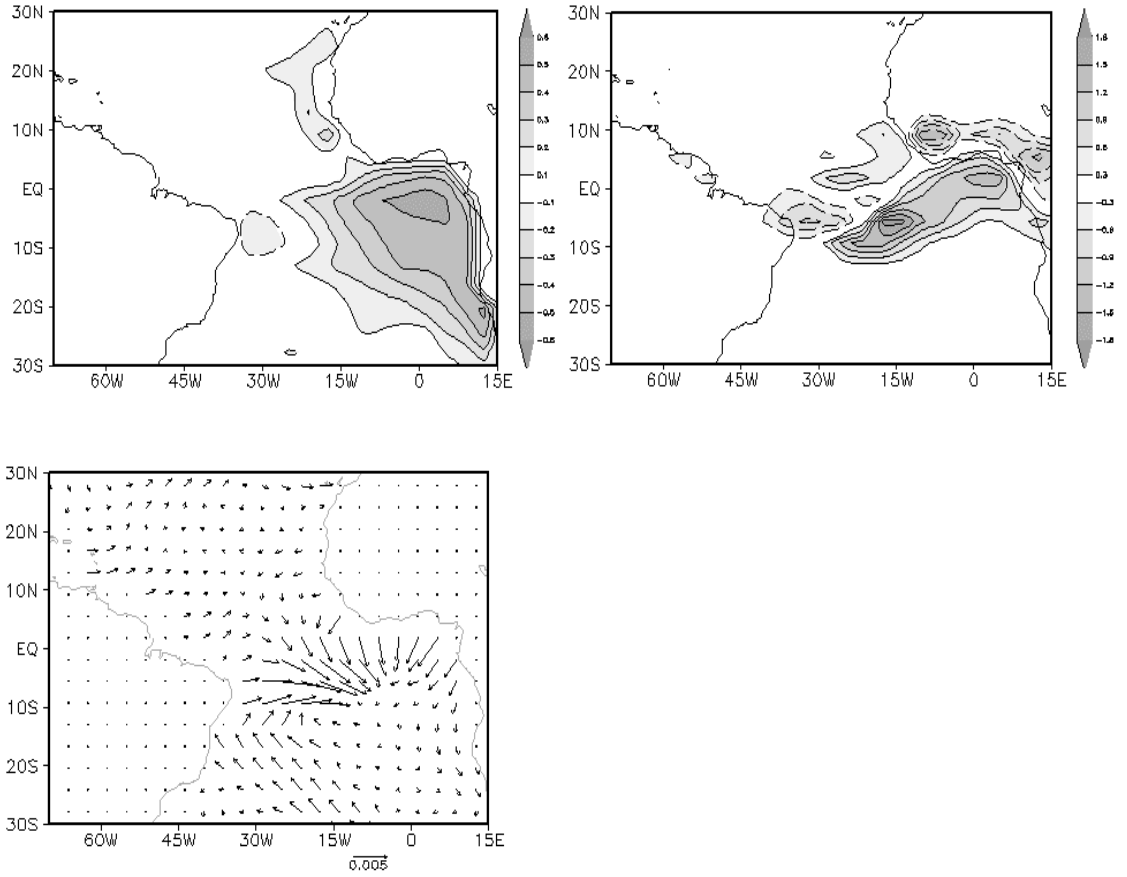

c

Fig. 1. Regression of the principle component (PC) of the equatorial cold tongue mode onto SST [^{0}C] (a), precipitation [mm day^{-1}](b) and wind stress[Nm^{-2}] (c). The patterns are normalized to one standard deviation of the PC. In this and following figures the solid and dashed contours indicate positive and negative values respectively. The zero contour is omitted.

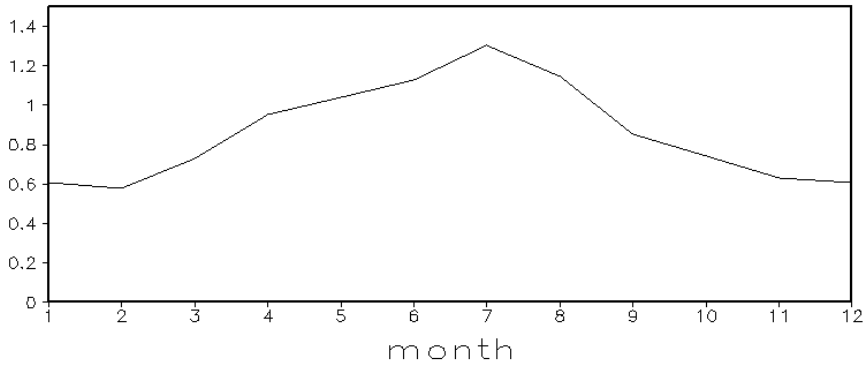

Fig. 2. Annual variation of the standard deviation of the PC of the equatorial cold tongue mode. The PC is normalized to one standard deviation.

a

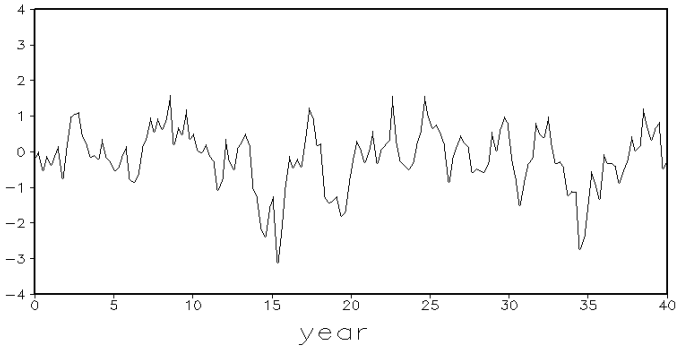

b

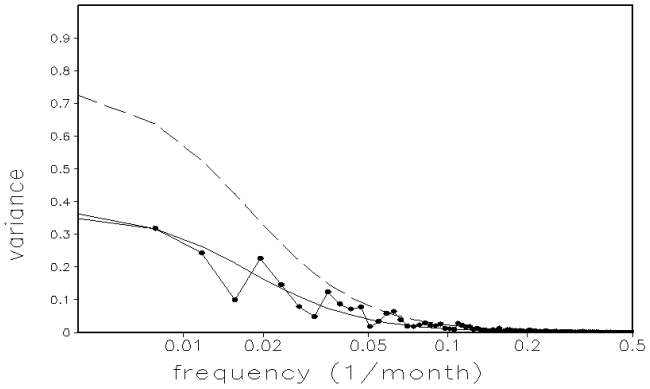

Fig. 3. **a**: Time series of PC of the SST of the cold tongue mode during the last 40 years **b**: Spectrum of **a** for the entire integration period of 80 years (black dots) together with the fitted AR(1) (red noise) process spectrum (solid line) and the 95% a priori confidence level (dashed line). The PC is normalized to one standard deviation.

a

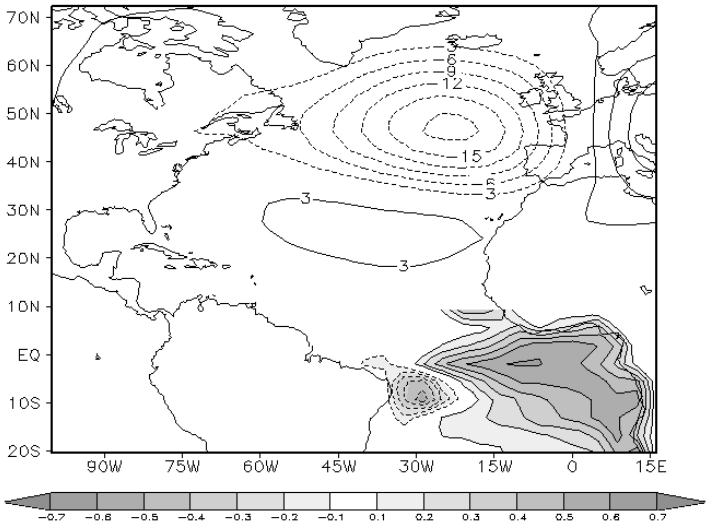

b

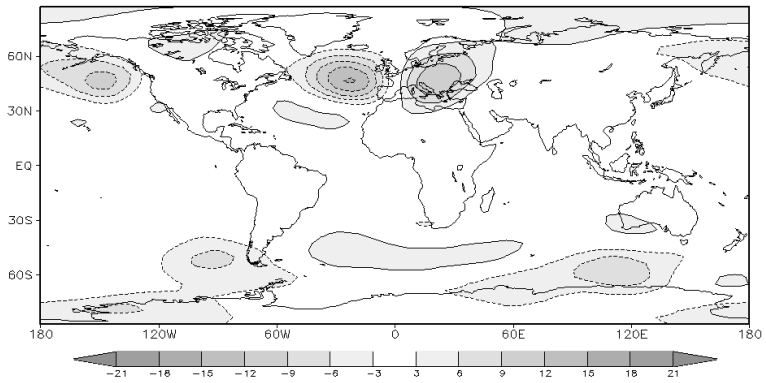

Fig. 4. **a**: Lagged MCA analysis of the 80-yr coupled run of tropical SST [^{0}C] (homogeneous map) during JAS (shaded) and Z500 [m] (heterogeneous map) during OND (contours). The explained variance is 46% and the cross correlation is 0.40

b: Regression of the PC of the cold tongue mode of JAS onto the Z500 [m] of OND.

The SST time series of the MCA analysis and the PC of the cold tongue mode are normalized to one standard deviation.

a b

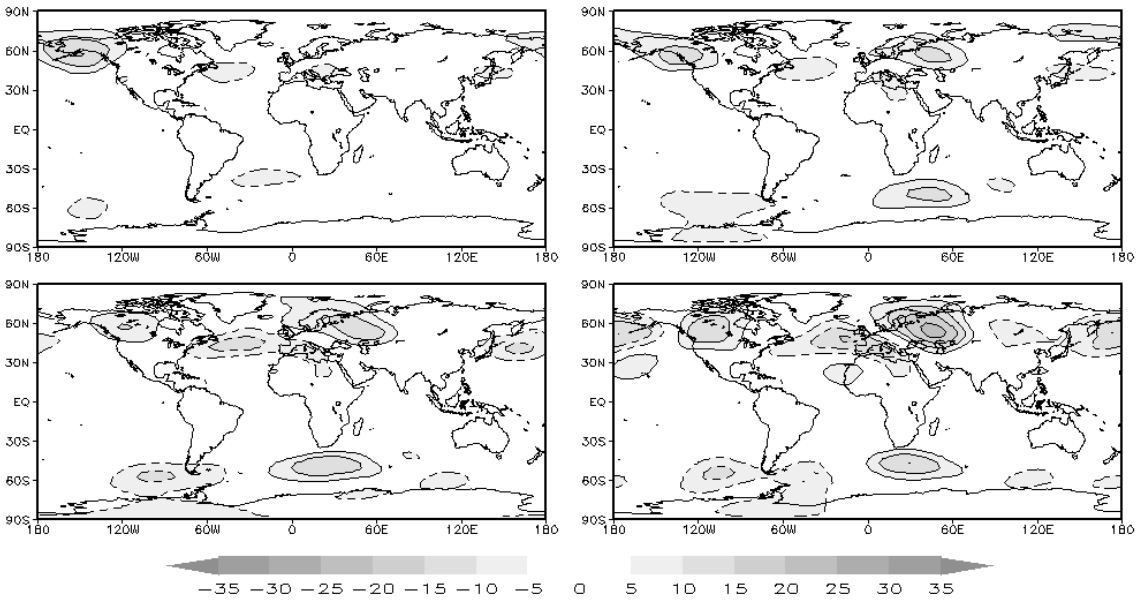

c d

Fig. 5. Z500 response in [m] to a 2 stdv anomaly of the cold tongue mode in the Q-flux experiment. The response is averaged over ASO (a), SON (b), OND(c), NDJ(d).

a b

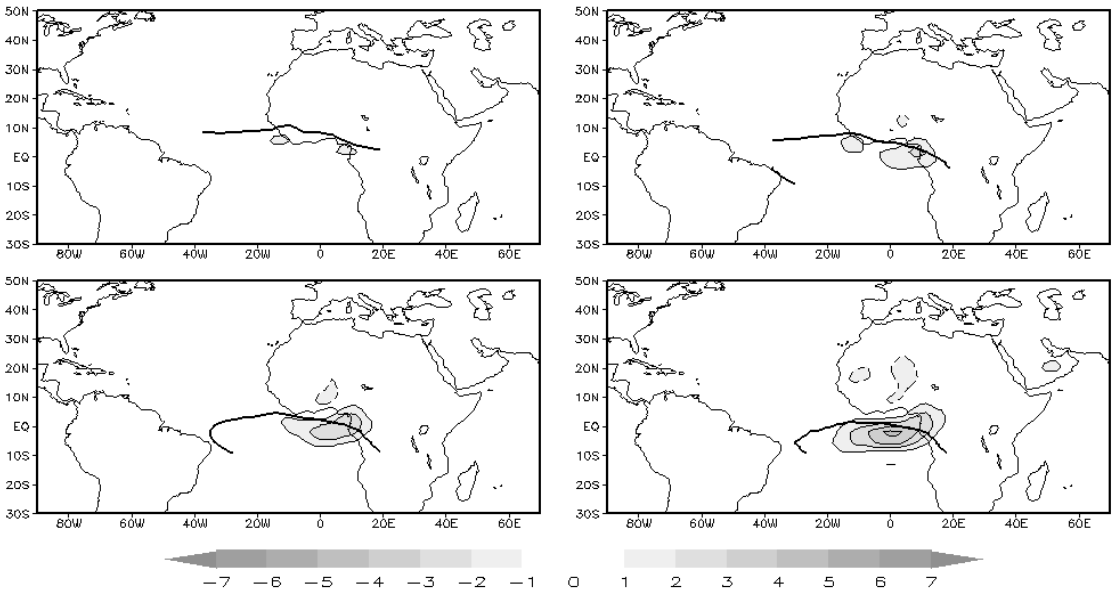

c d

Fig. 6. Anomalous divergence [10^{-6} s^{-1}] at 200 hPa in the Q-flux experiment during ASO(a), SON(b), OND(c) and NDJ(d). The solid line is the position of the ITCZ, which is computed as the line of zero meridional surface wind.

a b

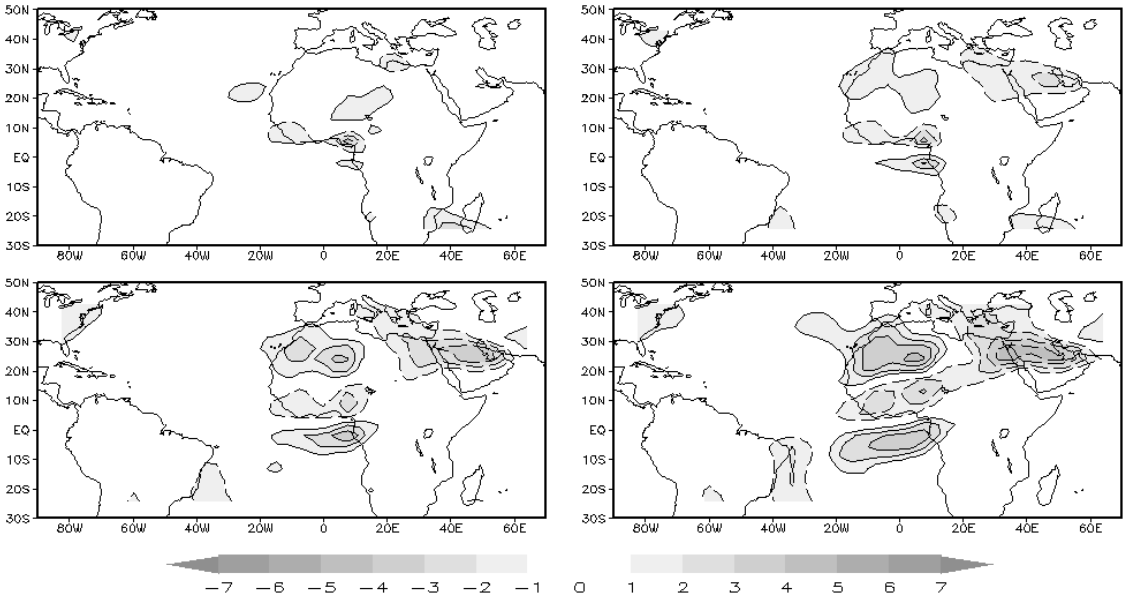

c d

Fig. 7. Anomalous Rossby wave source S [10^{-11} s^{-2}] at 200 hPa in the Q-flux experiment during ASO(a), SON(b), OND(c) and NDJ(d).

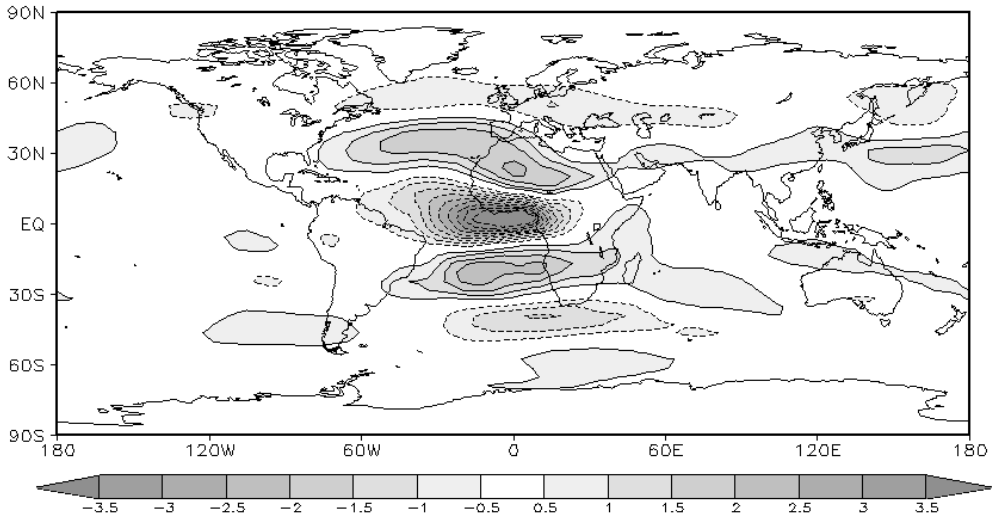

Fig. 8. Anomalous zonal wind U at 200 hPa [m] in the Q-flux experiment for OND.

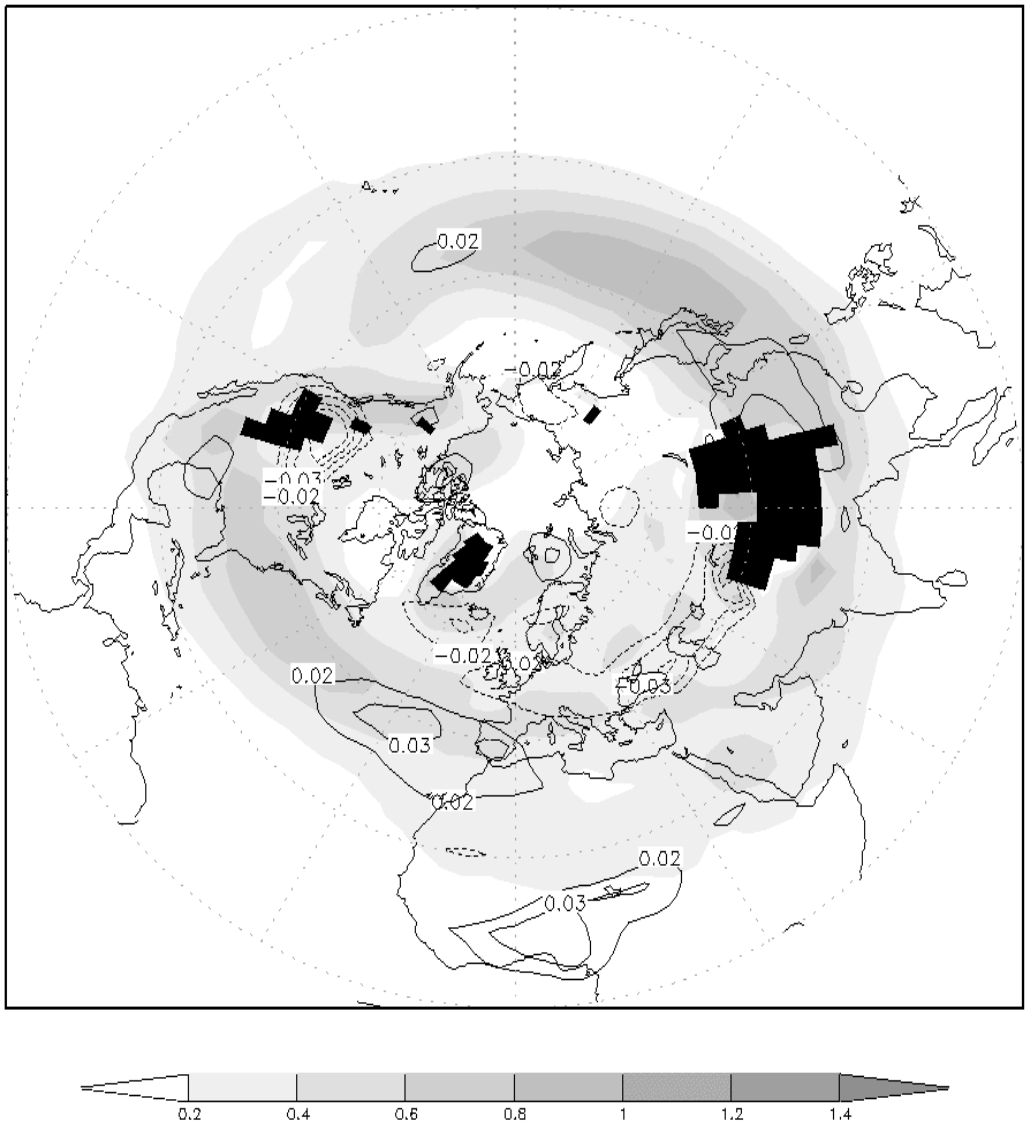

Fig. 9 Maximum Eady Growth rate σ_{BI} in 0.1 day^{-1} in the Q-flux experiment. Control (shaded) and anomalous (contours). Regions where the 850 hPa geopotential height is beneath the surface have been blacked out.

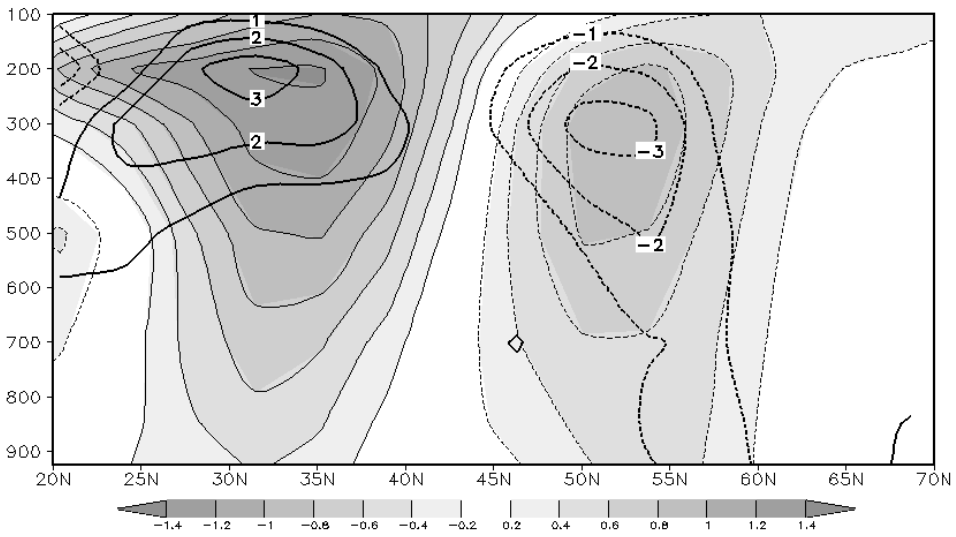

Fig. 10. Anomalous zonal wind u [m s^{-1}] (shaded) and meridional convergence of eddy momentum transport -d (u'v')/dy * T [m s^{-1}] (contours) zonally averaged over the Atlantic (50^{o}W-25^{o}E, 20^{o}S-70^{o}N). T is 14 days.

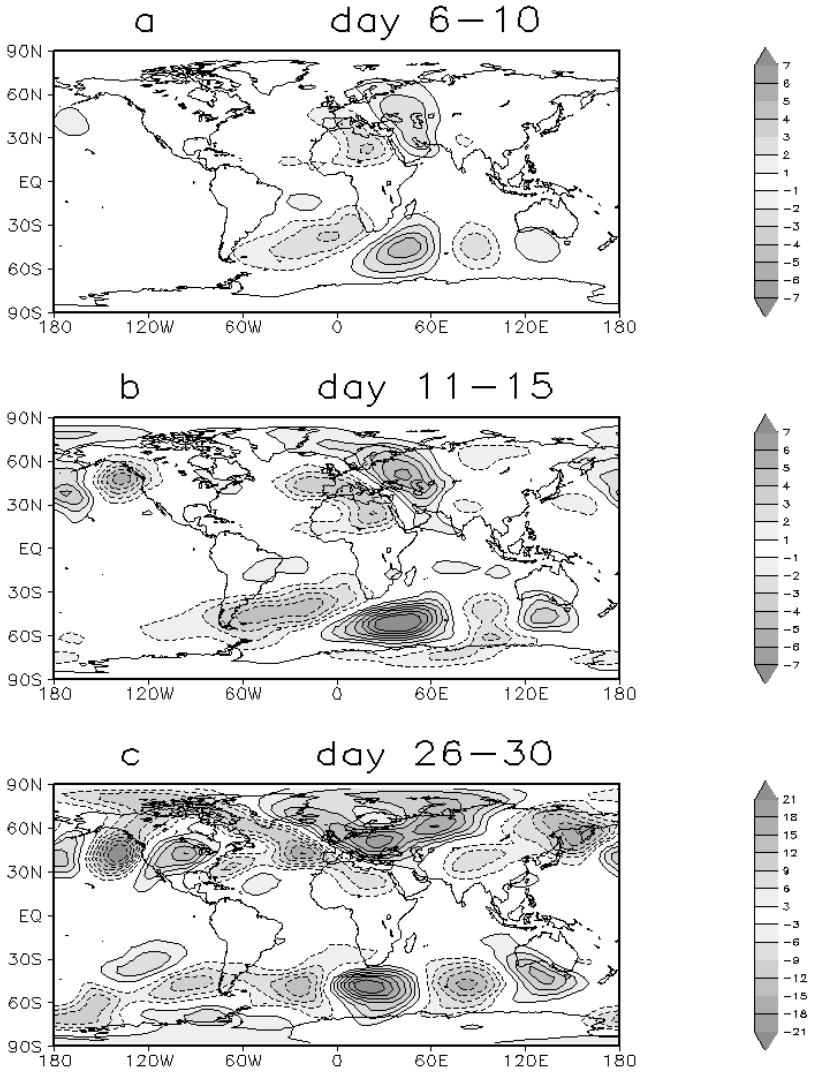

Fig. 11. Ensemble mean Z500 response [m] (200 members) of a positive cold tongue anomaly of 2 standard deviations in November: **a:** averaged over day 6-10 after the perturbation is switched on.; **b:** as a but now averaged over day 11-15 ; **c:** as a but now averaged over day 26-30.

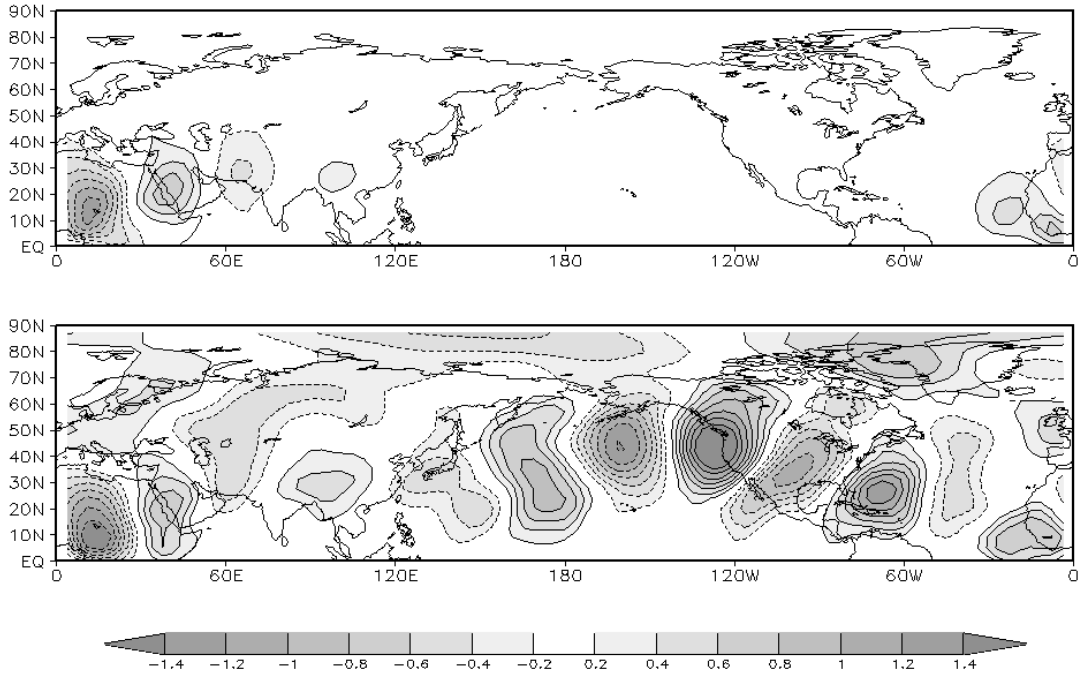

Fig. 12. Ensemble mean response of the non divergent v [m s^{-1}] at 300 hPa at day 7 (upper panel) and averaged over the period 16-30 days (lower panel).

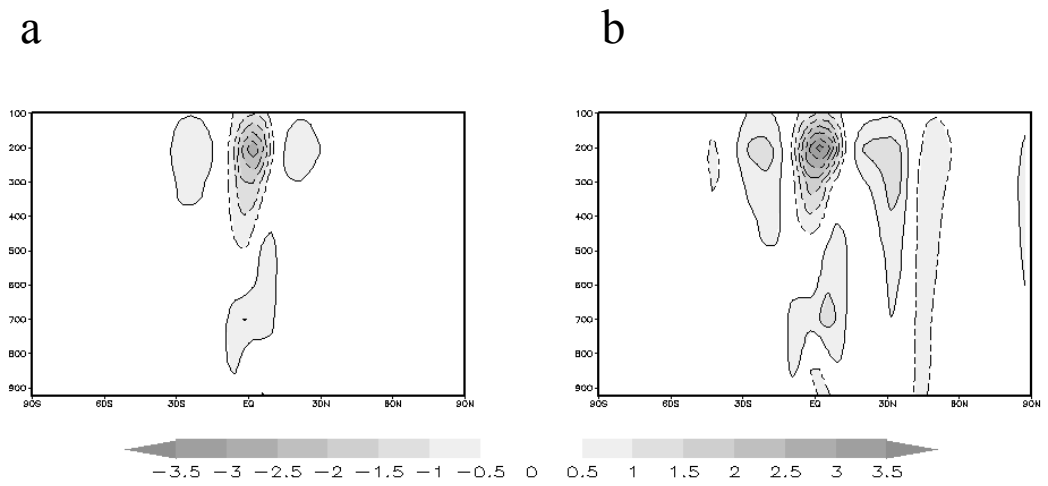

Fig. 13. Ensemble mean response of the zonal wind u [m s^{-1}] zonally averaged over the Atlantic (50^{o}W-25^{o}E, 20^{o}S-70^{o}N) averaged over day 11-15 (**a**) and day 26-30 (**b**).

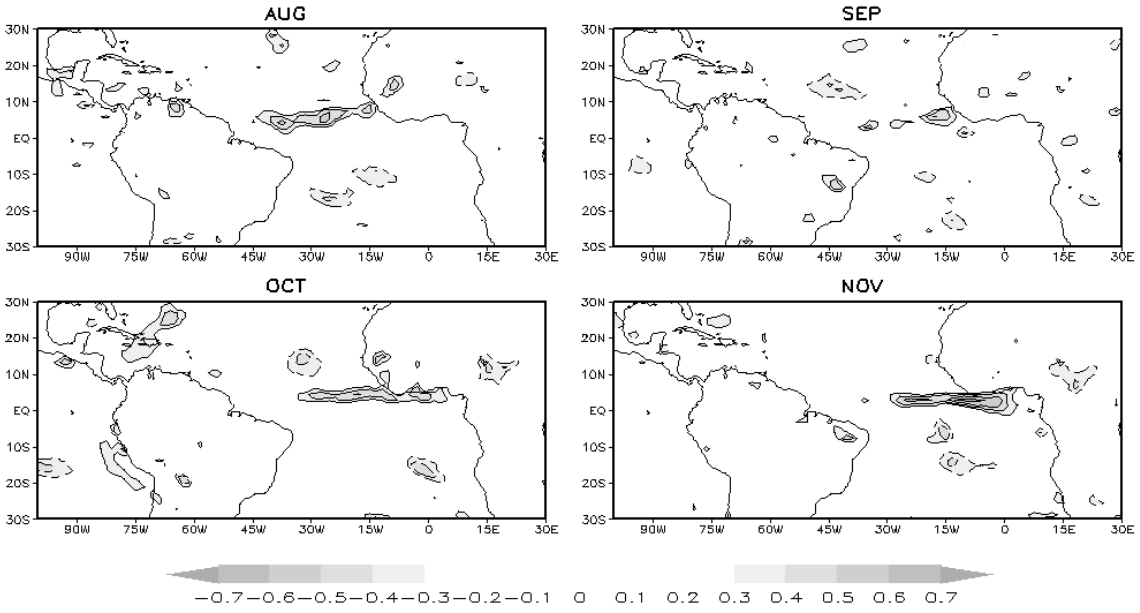

Fig. 14. Correlation of the ATL3 index with the 200 hPa divergence (ERA40 reanalysis) for the months August till November.

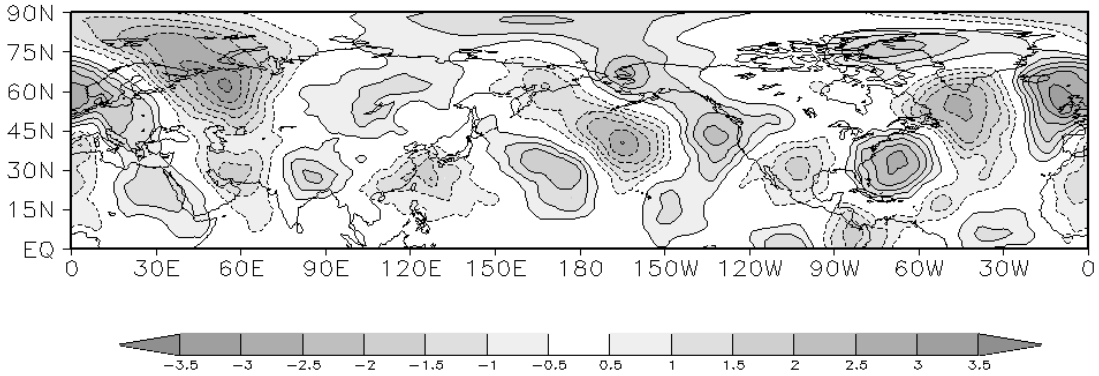

Fig. 15. Regression of the ATL3 index with the ERA40 merdional 300 hPa wind [m s^{-1}] for the period NDJ.